Journal of Analytical and Applied Pyrolysis 100 (2013) 26–32

Contents lists available at SciVerse ScienceDirect

Journal of Analytical and Applied Pyrolysis

journal homepage: www.elsevier.com/locate/jaap

TG–FTIR and Py–GC/MS analysis on pyrolysis and combustion of pine sawdust

Ningbo Gao[a,b], Aimin Li[a,*], Cui Quan[a], Lin Du[b], Yue Duan[b]

[a] School of Environmental Science & Technology, Dalian University of Technology, Key Laboratory of Industrial Ecology and Environmental Engineering, MOE, Dalian 116024, China
[b] Institute of Process Engineering, Chinese Academy of Sciences, State Key Laboratory of Multiphase Complex Systems, Beijing 100190, China

ARTICLE INFO

Article history:
Received 2 September 2012
Accepted 13 November 2012
Available online 24 December 2012

Keywords:
Pine sawdust
Pyrolysis
Combustion
TG–FTIR
Py–GC/MS

ABSTRACT

Pyrolysis and combustion of pine sawdust have been investigated by using thermogravimetric analyzer coupled with Fourier transform infrared spectrometry (TG–FTIR) analysis in this paper. Pyrolysis–gas chromatography and mass spectrometry (Py–GC/MS) analysis was employed to characterize subsequently the structure and composition of evolving gas in pine sawdust pyrolysis process. TG results showed that both pyrolysis and combustion of pine sawdust presented three weight loss stages, respectively. The apparent activation energy of pyrolysis reaction is 108.18 kJ mol^{-1} in temperature of 239–394 °C, while under combustion process which is 128.43 kJ mol^{-1} and 98.338 kJ mol^{-1} in 226–329 °C and 349–486 °C, respectively. The evolving gaseous products during the pyrolysis and combustion infrared spectrums such as H_2O, CH_4, CO, CO_2, phenol and alkane were found. Py–GC/MS results indicated that the main compounds of pine sawdust thermal decomposition were small molar gases, acetaldehyde, acetic acid, anhydride with formic and acetic anhydride. And possible formation pathways for main pyrolysis products were tentatively presented.

1. Introduction

As a potential energy resource, biomass energy is one of most important renewable energy. There are several ways (e.g. physical, thermal, chemical, and biological conversion) to generate energy from biomass [1]. Of all the different processes for biomass utilization, the pyrolysis and combustion are main thermal methods to optimize the conversion of the chemical energy of the fuel [2].

During biomass pyrolysis and combustion, it is necessary to know the possible thermal conversion mechanisms by which pyrolysis and combustion occurs in the different molecular fractions. This may allow us to control the process in order to obtain acceptable and reusable products [3]. The determination of kinetic parameters and process products gives us information on the thermal events occurring as well as the structure and composition of the materials [4].

Thermogravimetric analysis (TG) coupled with Fourier transform infrared (FTIR) analysis is a well established method for obtaining weight loss to study biomass thermal decomposition characteristics, reaction mechanisms and evolved products during pyrolysis and combustion. This method offers the potential for the non-destructive, simultaneous, real-time measurement of multiple gas phase compounds in complex mixture. Pyrolysis and combustion thermogravimetric analysis involves the sample thermal degradation in an inert and oxygen existing atmosphere, and the loss of the sample weight was recorded simultaneously at a uniform temperature ramping rate. Weight loss and calculated kinetic parameters are easily obtained from thermogravimetric analysis without the complex chemical reactions in the thermal degradation, and the evolved gases are detected in real-time and sensitively, which is an important and often a difficult task in many thermal applications. Extensive studies had carried out with thermogravimetric analyzer coupled with Fourier transform infrared spectrometry (TG–FTIR) for biomass and other materials thermal events [5–9].

Another way to study biomass pyrolysis components evolving is by quantitative pyrolysis–gas chromatography/mass spectrometry (Py–GC/MS). Py–GC/MS is an important technique for biomass characterization, because it involves not only the compositional information of the complex component macromolecules, but also the characteristics of volatile pyrolysis products. A number of aspects of Py–GC/MS used as a quantitative tool were discussed. And also Py–GC/MS has been shown to be a reliable analytical technique for the characteristics of biomass [10–12]. Fahmi et al. [12] determined the composition of the thermal degradation products of lignin with Py–GC/MS by the use of different biomass samples. Lu et al. [13] investigated the effect of Al/SBA-15 catalysts on biomass fast pyrolysis vapors by Py–GC/MS. Although analytical pyrolysis techniques were employed the portion of the sample which is pyrolitically volatile, comparative studies using TG–FTIR and Py-GC/MC are rare. In the present study, we quantify analysis the composition of gas evolved during the thermal degradation of pine sawdust.

* Corresponding author. Tel.: +86 411 84707448; fax: +86 411 84706679.
E-mail addresses: nbgao@dlut.edu.cn (N. Gao), leeam@dlut.edu.cn (A. Li).

0165-2370/$ – see front matter © 2012 Elsevier B.V. All rights reserved.
http://dx.doi.org/10.1016/j.jaap.2012.11.009

Table 1
Ultimate analysis of biomass (Air dry basis).

Materials	M[a]	Ash	C	H	O[b]	N	S
Pine sawdust	3.93	0.34	44.75	6.31	42.94	1.68	0.05

[a] Moisture.
[b] By difference.

The thermal decomposition of pine sawdust is investigated during pyrolysis and combustion process, respectively. TG–FTIR and Py–GC/MS experiments were performed to investigate how the thermal degradation of pine sawdust will affect the structure and composition of various products formed during the pyrolysis and combustion.

2. Experimental

2.1. Materials

The original material (pine sawdust) used in this study was collected from a timber mill in Dalian, China. The pine sawdust sample was ground to pass a 60-mesh screen. The carbon (C), hydrogen (H), nitrogen (N), sulphur (S) analyses of pine sawdust were performed on a CHNS/O analyzer (Elementar, VarioEL III, Germany), the ash value of the pine sawdust sample was measured by a automatic proximate analyzer (SDTGA5000, Sundy, China), oxygen (O) obtained by difference to 100%. ASTM standardized procedures were used to analyze for these properties. Table 1 shows the ultimate and proximate analysis of the used sample.

2.2. TG–FTIR analysis

The TG–FTIR simultaneous measurement for the on-line analysis of volatile compounds formed during TG runs consists of a thermogravimetric analyzer (TG209F1, Netzsch, Germany) coupled with a FTIR spectrophotometer (Vertex70, Bruker, Germany). In this study, approximately 10 mg of sample was heated in N_2 and air environment at 10 °C/min. First, the temperature was raised from ambient temperature to 120 °C to dry the sample for 10 min, and then to 700 °C for pyrolysis and combustion. The flow rate of carrier gas (N_2/air) was set at 30 mL/min. The differential thermogravimetric (DTG) curves were obtained by numerical derivation of the TG curves. The gas products released from the pyrolysis in TG were swept immediately to a cold gas cell for analysis by FTIR. The transfer line and gas cell were heated to 190 °C to prevent condensation of the produced gases. Resolution in FTIR was set at 4 cm^{-1}, spectrum scan frequency was 8 times per minute, and the spectral region was in 600–4000 cm^{-1}. The distribution of gaseous products from pyrolysis was analyzed, with respect to the changing of reaction temperatures from 120 to 700 °C.

2.3. Reaction kinetics of pyrolysis and combustion of pine sawdust

As a common method, the kinetics of pyrolysis and combustion of pine sawdust was largely described by first order Arrhenius law [14]. Coats-Redfern integral method [9] was used to determine the activation energy of the non-isothermal degradation of pine sawdust samples.

Thus rate equation for the kinetics analysis can be expressed as [15]:

$$\frac{d\alpha}{dt} = k(T)f(\alpha) \tag{1}$$

where α is the conversion ratio of pine sawdust feedstock at the time t (s), $f(\alpha)$ is differential form of the kinetic model. k is rate constant, which is given by the Arrhenius equation: $k = A\exp(-E/RT)$, A is a pre-exponential factor (min^{-1}), E is the activation energy (J mol^{-1}), T is the temperature of reaction (k), R is the universal gas constant (8.314 J mol^{-1} K^{-1}).

α can be defined as:

$$\alpha = \frac{(m_0 - m_t)}{(m_0 - m_f)} \tag{2}$$

where, m_t is the weight at any time t, and m_0 is the initial weight at the start of that stage, and m_f is the final weight at the end of that stage.

The reaction model in Eq. (1) can be expressed as:

$$f(\alpha) = 1 - \alpha \tag{3}$$

Under a constant heating rate $\beta = dT/dt$, the reaction equation may be expressed as following formula:

$$\frac{d\alpha}{dT} = \frac{A}{\beta}(1-\alpha)\exp\left(-\frac{E}{RT}\right) \tag{4}$$

According to the approximate expression of Coats–Redfern method (single heating-rate integral method), Eq. (4) can be re-arranged and integrated as follows:

$$\ln\left[\frac{-\ln(1-\alpha)}{T^2}\right] = \ln\left[\frac{AR}{\beta E}\left(1-\frac{2RT}{E}\right)\right] - \frac{E}{RT} \tag{5}$$

For most temperature region and E of pyrolysis and combustion reaction, $E \gg 2RT$, $(1-(2RT/E)) \approx 1$, so Eq. (5) can be simplified as

$$\ln\left[\frac{-\ln(1-\alpha)}{T^2}\right] = \ln\left(\frac{AR}{\beta E}\right) - \frac{E}{RT} \tag{6}$$

Eq. (6) gives a plot of $\ln[-\ln(1-\alpha)/T^2]$ versus T^{-1} for various heating conditions should yield a straight line, whose slope is $-E/R$ and Y intercept is $\ln(AR/\beta E)$. The value of α, and T at any times could be obtained from the experimental TG and DTG curves. Thus, the apparent activation energy E and the pre-exponential factor A, could be determined from the above method [16].

2.4. Py–GC/MS analysis

Pyrolysis-gas chromatography/mass spectrometry (Py–GC/MS) system was employed to separate and identify the pyrolysis volatiles. For this purpose, a Frontier PY-2020iD typed pyrolyzer (Japan) was directly attached to a gas chromatography/mass spectrometry (5890GC/5972MSD, Agilent). In the characterization process, the pyrolysis temperature of 600 °C was used. The chromatographic separation of the volatile products was performed using a Varian CP-Sil 24CB capillary quartz column (30 m × 0.25 mm, 0.25 μm, USA). Before the chromatograph separation, the temperature of the chromatographic column was progressively increased as follows: (i) 35 °C for 3 min; (ii) from 35 to 260 °C at a rate of 4 °C/min; (iii) the capillary column was maintained at 260 °C for about 40 min. Helium was used as carrier gas at a constant flow of 1.0 mL/min. The mass range used for the mass selective detector was 40–550 m/z. The decomposition products were identified by means of the comparison between the experimental mass spectrum and the mass spectrum library attached to the Py–GC/MS apparatus. The identification of each volatile products can be confirmed if the qualification percentage reaches 85% and even higher.

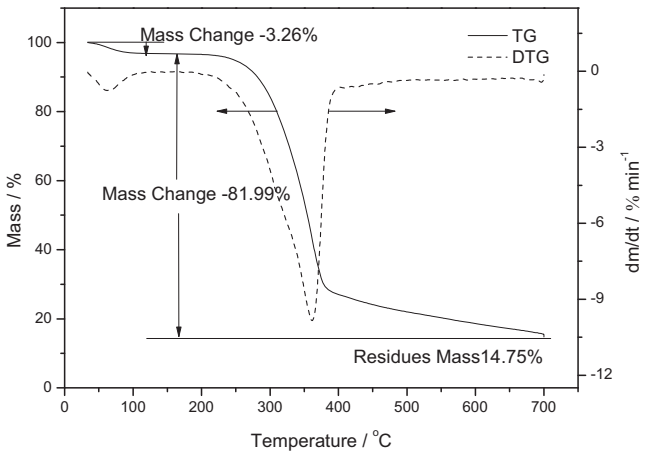

Fig. 1. TG and DTG curves for pine sawdust pyrolysis.

3. Results and discussion

3.1. Thermogravimetric analysis

The thermogravimetric curve and differential thermogravimetric curve during pyrolysis and combustion of pine sawdust at the heating rate of 10 °C min^{-1} are presented in Figs. 1 and 2 respectively. Three stages were found in pyrolysis process as shown in Fig. 1. The first stage (3.26% weight loss) was attributed to moisture evaporation from ambient temperature to 120 °C. The second stage is main weight loss between 200 and 405 °C with a sharp decrease on pine sawdust weight, and this stage might be associated with the hemicellulose decomposition, whereas the maximum value (occurred at 361 °C) is related to the maximum decomposition rate of the cellulose, a major wood component [17]. During the second stage about 73.25% of the total weight was rapidly decomposed. It is well known that the temperature range of decomposition for hemicelluloses is 225–350 °C, 325–375 °C for cellulose, and 250–500 °C for lignin [18]. It is a rough judgment for the main pine sawdust component decomposition. The last stage (405–700 °C) in pyrolysis is the further cracking process of pine sawdust residues due to lignin decomposition. Similar trends in mass loss rates were reported by Hu et al. [19] for cellulose. The weight loss was slight in this stage, and about 11.99% of the total weight was cracked at a lower rate. Finally, pine sawdust sample remained a solid residue (carbonaceous residues within inorganic solid particles) equal to 14.76% of its original mass. The total weight loss of 85.24% of sample weight was observed in the pyrolysis process. In this study, these three stages were assigned by using a broad classification.

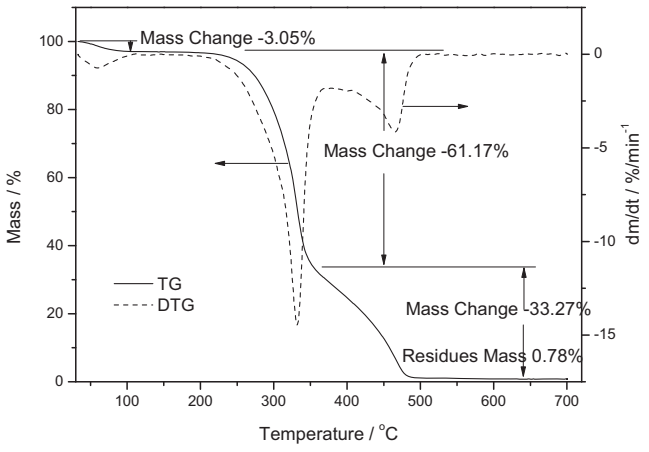

Fig. 2. TG and DTG curves for pine sawdust combustion.

Also three weight loss regions were presented in the whole TG curves of pine sawdust combustion (see in Fig. 2). The first two weight loss thermal decomposition of combustion is similar to that of pyrolysis between ambient temperature and 383 °C. About 3.05% of the total weight was lost for moisture evaporation in 30–113 °C. The major weight loss, about 66.72% of the total weight of pine sawdust sample, was due to pine sawdust volatilization and char oxidation process [20]. The peak at 465.7 °C between 383 and 500 °C is due to oxidization of carbonaceous residues within inorganic solid particles. The temperature range was in agreement with previous literature [21]. As the regions of volatiles release, char combustion and transformation are overlapping [22], it is difficult to accurately establish a distinct boundary among these thermal decomposition stages. It is possible to minimize the overlapping by applying much slower heating rate, for example 5 °C min^{-1}, or using a smaller sample [3].

3.2. Kinetic analysis

The activation energy and pre-exponential factors of non-isothermal analysis pine sawdust pyrolysis and combustion by TG–FTIR was presented in Table 2. Correlation coefficients indicated that the first order reaction model fits the experimental data very well. Combined with Figs. 1 and 2, one weight loss peak was observed in pyrolysis process during 239–394 °C, while two weight loss peaks were presented in combustion reaction in two small temperature ranges of 226–329 °C and 349–486 °C. The activation energy and frequency factor in pyrolysis reaction are 108.18 kJ mol^{-1} and 4.69×10^8 min^{-1} in temperature of 239–394 °C, respectively (Table 2). These results were in agreement with Singh et al. [9]. For the combustion runs, the activation energy and frequency factor of the first weight loss peak (in the temperature of 226–329 °C) are 128.43 kJ mol^{-1} and 8.20×10^{10} min^{-1}, while in the second weight loss, the values of activation energy and frequency factor are 98.338 kJ mol^{-1} and 3.84×10^6 min^{-1}, respectively. It can be seen that in the higher temperature range, the activation energy and frequency factor declined. Similar trend were observed in obvious studies [23]. The reason may be, during low temperature range, the volatiles evolved from pine sawdust covered the surface of samples and the formed carbonaceous char might form a physical barrier, which insulate heat from the flame and to prevent the diffusion of combustible gases. Thus, the rate of mass and heat transfer was hindered, and the reaction activity was declined accordingly and more energy needed to activate the reaction. As the temperature increases, the primary reaction might be changed as activated char combustion, and the activation energy declines.

3.3. Three dimension FTIR spectra analysis

3.3.1. Pyrolysis analysis

The 3D FTIR spectrum of the evolved gases of pine sawdust pyrolysis including information on infrared absorbance, wave number and time are shown in Fig. 3. In this figure, it can be concluded that most of the gas was evolved between 25 and 40 min. Several FTIR spectra of all the pyrolysis volatile products were selected for primary analysis at different times. In accordance with the TG data in Fig. 1, the characteristics of spectra obtained at 236 °C, 282 °C, 318 °C, 345 °C and 359 °C are shown in Fig. 4. The following gaseous species were quantified by the spectra: carbon dioxide, carbon monoxide, methane, water, phenols, and other paraffin gas (Fig. 5).

As seen in Fig. 4, the evolved gases of pine sawdust pyrolysis were identified by their characteristic absorbance. In the initial pyrolysis stage (at 236 °C), CO_2 was presented in wave numbers

Table 2
The kinetic analysis of biomass pyrolysis and combustion.

Reaction	Temperature range (°C)	E (kJ mol^{-1})	A (min^{-1})	Correlation coefficient, R
Pyrolysis	239–394	108.18	4.69×10^8	0.986
Combustion	226–329	128.43	8.20×10^{10}	0.980
	349–486	98.338	3.84×10^6	0.981

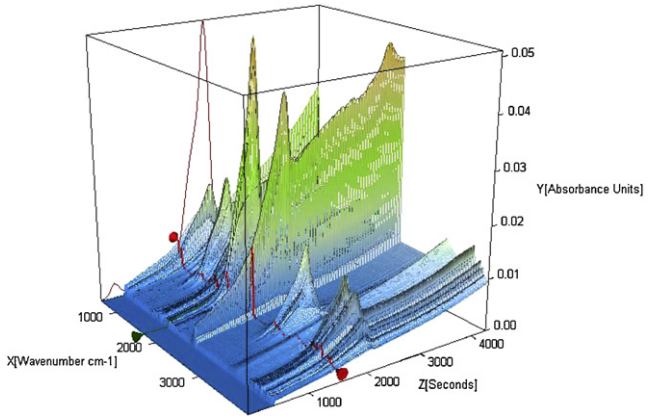

Fig. 3. 3D TG/FTIR diagram of pine sawdust pyrolysis.

2400–2260 cm^{-1}, nonconspicuous peak was shown in the wave numbers 4000–3400 cm^{-1}, and 1900–1300 cm^{-1}, which means very little H_2O evolved. With pyrolysis temperature increased to 282 °C, very litter C—O asymmetric stretching absorbance wave appeared in the wave of 1131–1077 cm^{-1}, indicating the existence of alcohols [24]. The C=O stretching absorbance peaks in the region of 1900–1650 cm^{-1} were representative of aldehyde or organic acid. As the pyrolysis temperature reached 318 °C, absorption wave in 3000–2700 cm^{-1}, related to C—H asymmetric stretching for CH_4 and a band in 3600–3050 cm^{-1} due to O—H stretching of water were also observed. The similar infrared (IR) absorbance of pine sawdust pyrolysis was observed at the temperature of 345 and 359 °C, the absorbance wave mentioned above was enhanced to some extent with the temperature increases.

According to the widely used Lambert–Beer law, the absorption spectrum at a specific wave number is linearly dependent on gas concentration [25]. Thus the variation of absorbance in the whole pyrolysis process reflects the concentration trend of the gas species. Fig. 5 shows the evolution of gaseous products with temperature increases during pine sawdust pyrolysis. The gases evolution was mainly concentrated between 240 and 400 °C, the release of CO, CH_4, H_2O, and aldehydes and alkane compounds were in agreement with weight loss thermogravimetric data. Carbon monoxide was one of the decomposition products of ether groups, which originate from the ether bridges of lignin subunits connection and/or the ether compounds in secondary cracking of volatiles. CH_4 formed from the cracking of a weakly bonded methoxy group —OCH_3— and the break of having higher bond energy of methylene group —CH_2— [26]. In the temperatures between 100 and 500 °C, H_2O released mainly from the evolution of bulk water, bound water and crystallization water in mineral substance in pine sawdust sample. With the temperature increases, the pyrolysis water forms also from the cracking or reaction of oxygen functional groups occurred in pine sawdust pyrolysis. A different trend of the carbon dioxide (at wave numbers 2358 cm^{-1}) was observed that the content increases with increase in temperature and reached the maximum peak at 360 °C. As the temperature exceeded 400 °C, the decreased CO_2 in the temperature of 360–400 °C, presented an increasing tendency up to 700 °C. This is due to the CO_2 releases from volatile matter below 400 °C. As the temperature increases, the polymerization reaction of coking in solid phase is primary reaction, and this process accompanies the emission of low concentration CO_2. At the end of coking polymerization reaction, the absorbance intensity of CO_2 will be decrease.

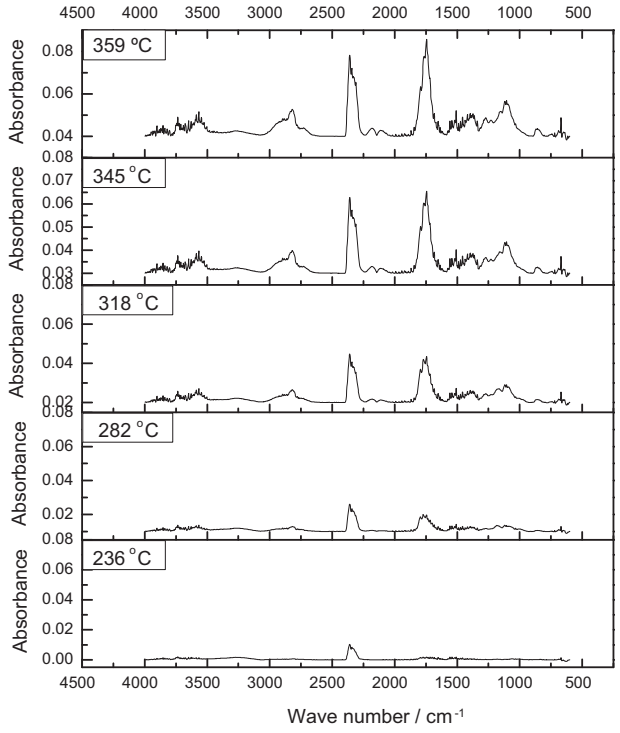

Fig. 4. FTIR spectra for the volatile components in vapor phase of pine sawdust pyrolysis at each mass loss.

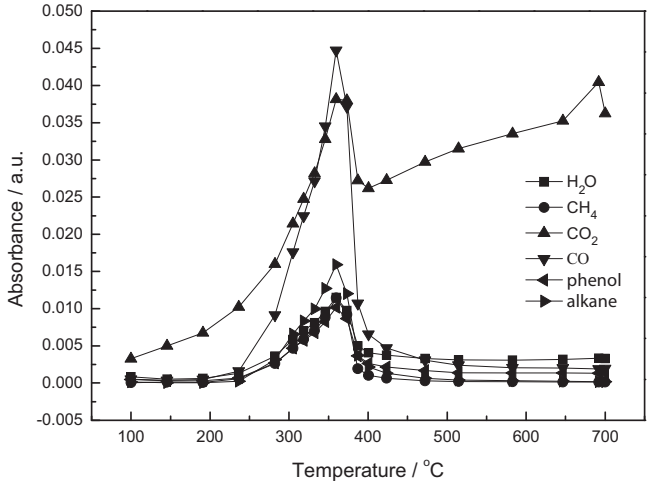

Fig. 5. Evolution of gaseous products with increasing temperature during pine sawdust pyrolysis.

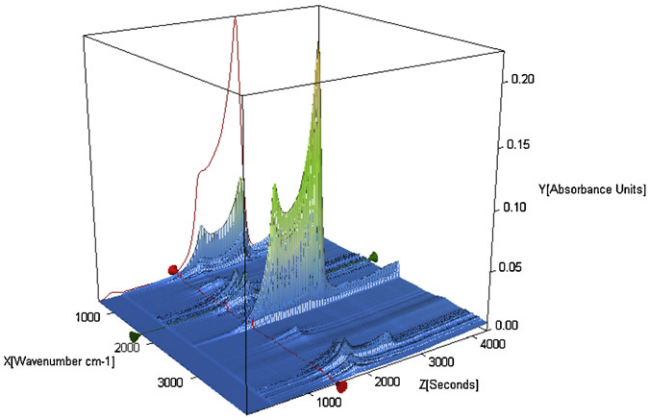

Fig. 6. 3D TG/FTIR diagram of pine sawdust combustion.

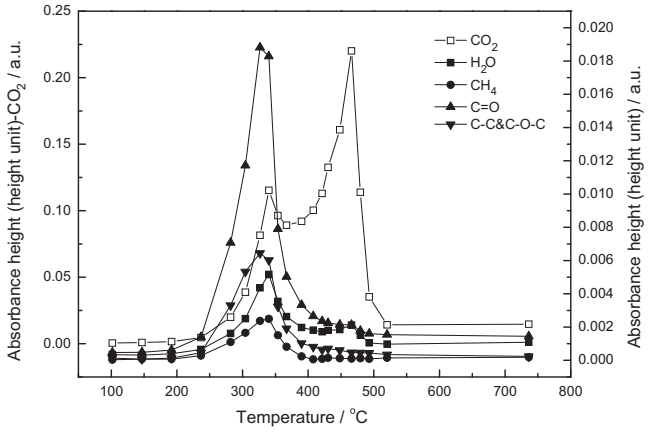

Fig. 8. Evolution of gaseous products with increasing temperature during pine sawdust combustion.

3.3.2. Combustion analysis

Fig. 6 is the plot of the 3D FTIR spectrum of the evolved gases of pine sawdust combustion. In this figure, it can be observed that two clear reaction stages exist in combustion process. The first one occurred between 1200 and 1900 s, the absorbance wave of evolved gas is obvious and the maximum peak at the temperature of 320 °C. The second reaction stage appeared in 2100–2300 s, and the 3D IR spectrum presents intense absorbance peaks with the maximum value at 465 °C. After 3120 s, the absorbance wave stabilized gradually. The appearance of absorbance wave is in agreement with weight loss in the TG curve of pine sawdust combustion (Fig. 2).

The changes in the FTIR spectra (4000–600 cm^{-1}) of evolved gases at different temperature during pine sawdust combustion were shown in Fig. 7. Five spectra ranges were selected for primary analysis in this study. Water was generated by the cleavage of aliphatic hydroxyl groups, which was and confirmed by the appearance of bands at 4000–3500 cm^{-1}. The characteristic infrared absorbance in the wave number of 3000–2730 cm^{-1} indicated the existence of methane. As carbon dioxide has a wave number 2400–2260 cm^{-1}, carbon monoxide was found in wave number 2260–1990 cm^{-1} in spectrum. Absorption bands at 1900–1660 cm^{-1} were related to C=O stretching for aldehyde or ketone compounds. Absorption bands at 1500 and 950 cm^{-1} were related to C—O—C bend stretching for the groups of phenols, ethers or esters, and absorptions at 900 and 650 cm^{-1} were assigned to C—H stretching for aromatic hydrocarbons. Methane, carbon monoxide, and the compounds of the bond of C=O and esters increased when the temperature were higher than 191 °C, but started to decrease above 340 °C. However, water and carbon dioxide reached the highest intensity at 468 °C, and then gradually decreased. These results indicated that CH_4, CO, esters and carbonyl groups were formed at around 191 °C and were cracked at above 340 °C. With the oxidized reaction developed in deep, the amount of CO_2 and H_2O were generated in maximum at 468 °C and then declined with the consumption of evolved gas.

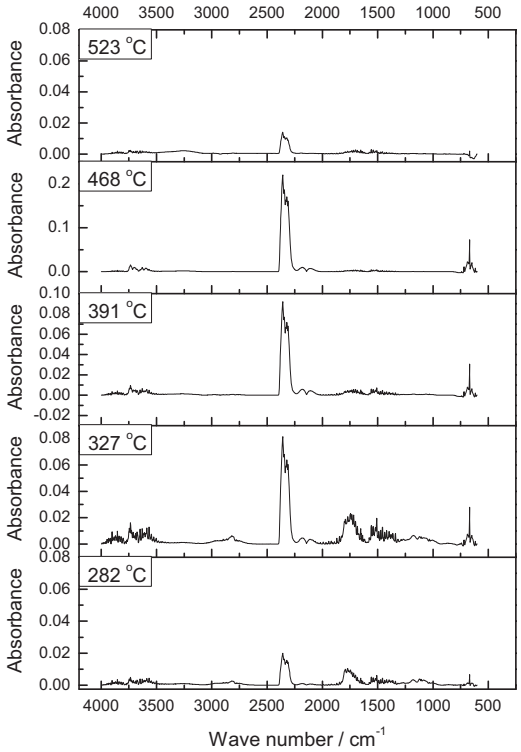

Fig. 7. FTIR spectra for the volatile components vapor phase in of pine sawdust combustion at each mass loss.

Besides the composition of combustion product was identified, the distribution of each evolved gases against time and temperature can be obtained. The evolution of gaseous products under various temperatures during pine sawdust combustion was shown in Fig. 8. Except for carbon dioxide appears two conspicuous absorbance peaks, other product gases such as CH_4, H_2O, esters, carbonyl groups and aromatic hydrocarbons show one distinct peak. The delay and smearing effect of spectral signal were disagreement with the trend of TG curve. This might be due to the transferring retardation and the inverse mixing diffusion of evolved gases, which caused the delay and deforming of spectral signal. Chen had reported that the flow rate of carrier gas in the range of 70–100 mL/min, the delay and smearing effect of the spectral signal intensity decrease remarkably [27]. At the first stage of the temperatures between 100 and 420 °C, the curves of evolved gases (Fig. 8) revealed the presence of CO, H_2O and CO_2, as well as small amounts of some organic volatile compounds such as aldehydes and acids (C=O), alcohols and phenols (C—O—C), alkanes (C—C), alkenes (C=C) and aromatic hydrocarbon. In this period, carbonyl group organic compounds begin to release violently. This might be due to the aldehydes, ketones and esters cracked by cellulose in the primary reaction. Methane was evolved by the cracking of methoxyl and methyl (OCH_3— and CH_3—). The methylene group —CH_2— also generated CH_4 at high temperatures [25]. As temperatures increase to 520 °C (second stage), all evolved gases expect for CO_2 gradually disappeared. The nonconspicuous methane evolution indicated that it was not favorable to produce CH_4 at higher temperatures. The weakly peaks of H_2O, alkanes (C—C) and phenols (C—O—C) compounds showed little gases forming in this stage. Large amount of

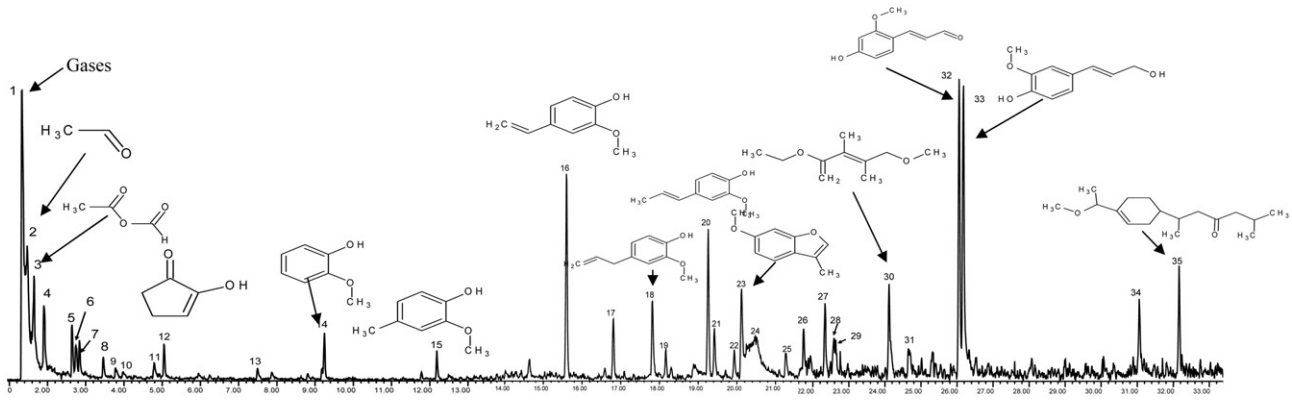

Fig. 9. TIC obtained by Py–GC/MS of pine sawdust. Peaks were characterized in Table 3.

CO_2 was produced from the cellulose and lignin cracking, volatiles and carbonized substrate (char) burning in this temperature range. Due to insufficient amount of oxygen, the pine sawdust combustion process could not be completed in the lower temperature range. Higher excess air and improved mixing may be helpful for the further oxidation of the large molecular organics and carbonized substrate [3].

3.4. Py–GC/MS analysis

To investigate the formation of main components of products in pine sawdust pyrolysis process, pyrolysis gas chromatography and mass spectrometry (Py–GC/MS) analysis on the pine sawdust have been conducted. Compared the mass spectra fragmentation pattern with the PerkinElmer NIST library and published data, the highest likelihood of compounds identification were obtained. The total ion count (TIC) of evolved gases from pine sawdust pyrolysis is depicted in Fig. 9. A total of 35 main compounds were identified, and the peaks of TIC were characterized in Table 3. The main compounds with the corresponding % area identified were gases (1, 27.29%, here the first number denote the peak number, the same as following), acetaldehyde (2, 11.60%), acetic acid, anhydride with formic (3, 11.47%), acetic anhydride (4, 5.81%), 4-ethenyl-2-methoxyphenol (16, 3.31%), 1,6-anhydro-á-D-glucopyranose (levoglucosan) (24, 3.30%), 2-methoxyphenol (14, 3.00%), cyclohexanone (12, 2.00%), acetic anhydride (5,2.86%), 2-methoxy-4-(1-propenyl)- phenol (20, 2.42%), 4-((1E)-3-hydroxy-1-propenyl)-2-methoxypheno (31, 2.38%), acetic anhydride (7, 2.14%), succinaldehyde (6, 2.06%).

Among the compounds, acetic acid was generated from elimination of the acetyl groups originally linked to the xylose unit

Table 3
Analytical results of chemical constituents of 550 °C pyrolysis products of pine sawdust.

Label	t_R (min)	Peak area %	Compound	Molecular formula
1	1.334	27.29	Gases	–
2	1.469	11.60	Acetaldehyde	C_2H_4O
3	1.647	11.47	Acetic acid, anhydride with formic	$C_3H_4O_3$
4	1.905	5.81	Acetic anhydride	$C_4H_6O_3$
5	2.642	2.86	Acetic anhydride	$C_4H_6O_3$
6	2.743	2.06	Succinaldehyde	$C_4H_6O_2$
7	2.832	2.14	Acetic anhydride	$C_4H_6O_3$
8	3.458	1.43	Furfural	$C_5H_4O_2$
9	3.782	0.87	Butyraldehyde	C_4H_8O
10	3.972	0.74	Cyclobutanol	C_4H_8O
11	4.788	1.30	2(3H)-Furanone furan-2(3*H*)-one	$C_4H_4O_2$
12	5.045	2.00	Cyclohexanone	$C_6H_8O_2$
13	7.493	0.85	3-Methyl-1,2-cyclopentanedione	$C_6H_8O_2$
14	9.248	3.00	2-Methoxyphenol	$C_7H_8O_2$
15	12.187	1.54	2-Methoxy-4-methylphenol	$C_8H_{10}O_2$
16	15.596	3.31	4-Ethenyl-2-methoxyphenol	$C_9H_{10}O_2$
17	16.815	1.05	Eugenol	$C_{10}H_{12}O_2$
18	17.821	1.51	Vanillin	$C_8H_8O_3$
19	18.167	0.58	2-Methoxy-4-(1-propenyl)- Phenol	$C_{10}H_{12}O_2$
20	19.262	2.42	2-Methoxy-4-(1-propenyl)-phenol	$C_{10}H_{12}O_2$
21	19.419	1.05	2-Methoxy-4-propyl-phenol	$C_{10}H_{14}O_2$
22	19.933	0.57	6-Methoxy-3-methylbenzofuran	$C_{10}H_{10}O_2$
23	20.123	1.86	1-(4-Methyl-3-methoxyphenyl)-ethanone	$C_9H_{12}O_2$
24	20.481	3.30	1,6-Anhydro-á-D-glucopyranose (levoglucosan)	$C_6H_{10}O_5$
25	21.274	0.64	4-Hydroxy-3-methoxyphenylacetone	$C_{10}H_{12}O_3$
26	21.744	0.45	1,2-Dimethoxy-4-(2-propenyl)- benzene	$C_{11}H_{14}O_2$
27	22.336	0.66	Coniferyl alcohol	$C_{10}H_{12}O_3$
28	22.638	0.39	1-Propanone, 3-hydroxy-1-(4-hydroxy-3-methoxyphenyl)	$C_{10}H_{18}O_4$
29	24.113	0.94	Nonanoic acid, 6-phenyl-, methyl ester	$C_{16}H_{30}O_2$
30	24.683	0.32	Methyl-(2-hydoxy-3-ethoxy-benzyl)ether	$C_{10}H_{20}O_3$
31	26.058	2.38	4-((1E)-3-Hydroxy-1-propenyl)-2-methoxypheno	$C_{10}H_{12}O_3$
32	26.181	1.83	4-Hydroxy-2-	$C_{10}H_{16}O_3$
33	31.054	0.85	Coniferyl alcohol	$C_{10}H_{12}O_3$
34	32.161	0.95	n-Hexadecanoic acid	$C_{16}H_{32}O_2$
35	32.161	1.00	Todomatuic acid	$C_{16}H_{26}O_3$

[28]. The breakdown of glycosidic bonds and the rearrangement of cellulose monomer would result in the formation of 1,6-anhydro-á-D-glucopyranose (levoglucosan). And cyclohexanone was produced by levoglucosan dehydration. In the pyrolysis process, the dehydration of glucose groups, hemicellulose and lignin occurred in the range of 150–240 °C, 225–325 °C and 250–500 °C, respectively [29,30]. So, it can be inferred that most of glucose had been cracked at 550 °C. The ketones such as cyclohexanone(12), 3-methyl-1,2-cyclopentanedione (13), 1-(4-methyl-3-methoxyphenyl)-ethanone (23) and 4-hydroxy-3-methoxyphenylacetone (25) were formed by breaking the molecule bonds between C_2 and C_3 of glucose monomer and by opening the hemiacetals groups loop [31]. Phenolic organic compounds such as compound labels (14, 15, 16, 17, 18, 19, 20, 21 and 26) were produced by lignin deconstruction [32]. The main phenylpropanoid monomers in lignin and the bonds of C—C and C—O in many unstable branched-chain alkyl groups, such as methoxy, aliphatic hydroxyl, were cracked first, while these bonds in aromatic were relatively stable [33]. Other compounds in pine sawdust pyrolysis, such as furfural (8), 6-methoxy-3-methylbenzofuran (22), 1-(4-methyl-3-methoxyphenyl)-ethanone (23), were also produced from cellulose and hemicellulose [34].

Acetic acid is the typical product of hemicellulose pyrolysis. In the early stage of hemicellulose decomposition, the fracture of 4-O-methyl-D-glucuronic acid base caused the formation of acetic acid due to carboxyl cracking. Additionally, the broken joint bonds C-5 and O-1 or C-2 and O-1 of arabinose in the location of xylose base O-2 or O-3 also formed acetic acid [32]. Ketone and aldehyde compounds are the main products of secondary volatiles, whose small molecular products were derived from single sugar ring breakdown. The secondary cracking and unsaturated bonds condensation of aldehydes and ketones with stronger activity occurred with temperature increase. Furans organics were formed from the reactions of 4-O-methyl-D-glucuronic acid in branched chain of the xylan, also can be produced by the dehydration reaction of D-xylose monomer. Aromatics were derived from the breakdown of bonds connecting lignin to hemicellulose, and in this process, the reactions of condensation, polycondensation and cyclization occurred in primary products at higher temperature range [35].

4. Conclusions

The properties and characteristics of pyrolysis and combustion of pine sawdust were investigated by TG–FTIR. The kinetics parameters of pine sawdust determined by thermogravimetric data were close to literature values. Both the pyrolysis and combustion process of pine sawdust can be divided into three stages. The activation energy of pine sawdust pyrolysis is 108.18 kJ mol^{-1} during 239–394 °C, and the values were is 128.43 kJ mol^{-1} and 98.338 kJ mol^{-1} during 226–329 °C and 349–486 °C in combustion process, respectively. Most of the gases evolving occurred in the second stage in pyrolysis, and in the second and third stages in combustion. H_2O, CO_2, CO, CH_4, phenols, and other paraffin gas were identified by FTIR spectra. The Py–GC/MS analysis indicated that gases, acetaldehyde, acetic acid, anhydride with formic and acetic anhydride were the main high-molecular-weight decomposition products.

Acknowledgments

The work cited in this paper was supported by the National Natural Science Foundation of China (NSFC) (51006018), China Postdoctoral Science Foundation (no. 20090451264) and by an open foundation of State Key Laboratory of Multiphase Complex Systems (no. MPCS-2011-D-11).

References

[1] A.C.C. Chang, H. Chang, F. Lin, K. Lin, C. Chen, International Journal of Hydrogen Energy 36 (2011) 14252.
[2] A.V. Bridgwater, Chemical Engineering Journal 91 (2003) 87.
[3] G. Zheng, J.A. Koziński, Fuel 79 (2000) 181.
[4] J.A. Conesa, A. Domene, Thermochimica Acta 523 (2011) 176.
[5] T. Ahamad, S.M. Alshehri, Journal of Hazardous Materials 199–200 (2012) 200.
[6] L. Tao, G.-B. Zhao, J. Qian, Y.-k. Qin, Journal of Hazardous Materials 175 (2010) 754.
[7] S.-B. Lee, O. Fasina, Journal of Analytical and Applied Pyrolysis 86 (2009) 39.
[8] R. Bassilakis, R.M. Carangelo, M.A. Wójtowicz, Fuel 80 (2001) 1765.
[9] S. Singh, C. Wu, P.T. Williams, Journal of Analytical and Applied Pyrolysis (2012), 10.1016/j.jaap.2011.11.011.
[10] A. Alves, M. Schwanninger, H. Pereira, J. Rodrigues, Journal of Analytical and Applied Pyrolysis 76 (2006) 209.
[11] J.W. Choi, O. Faix, D. Meier, Holzforschung 55 (2001) 185.
[12] R. Fahmi, A.V. Bridgwater, S.C. Thain, I.S. Donnison, P.M. Morris, N. Yates, Journal of Analytical and Applied Pyrolysis 80 (2007) 16.
[13] Q. Lu, W. Li, D. Zhang, X. Zhu, Journal of Analytical and Applied Pyrolysis 84 (2009) 131.
[14] Y.F. Huang, W.H. Kuan, P.T. Chiueh, S.L. Lo, Bioresource Technology 102 (2011) 3527.
[15] J.H. Chen, K.S. Chen, L.Y. Tong, Journal of Hazardous Materials 84 (2001) 43.
[16] N. Gao, A. Li, W. Li, Waste Management & Research 27 (2009) 242.
[17] C.A. Ulloa, A.L. Gordon, X.A. García, Fuel Processing Technology 90 (2009) 583.
[18] W. Thanasit, T. Nakorn, Bioresource Technology 101 (2010) 5638.
[19] S. Hu, A. Jess, M. Xu, Fuel 86 (2007) 2778.
[20] N. Aghamohammadi, N.M. Nik Sulaiman, M.K. Aroua, Biomass and Bioenergy 35 (2011) 3884.
[21] M.V. Gil, D. Casal, C. Pevida, J.J. Pis, F. Rubiera, Bioresource Technology 101 (2010) 5601.
[22] R.G. Saade, J.A. Koziński, Journal of Analytical and Applied Pyrolysis 45 (1998) 9.
[23] Z. Yu, X. Ma, A. Liu, Biomass and Bioenergy 32 (2008) 1046.
[24] D.K. Shen, S. Gu, A.V. Bridgwater, Journal of Analytical and Applied Pyrolysis 87 (2010) 199.
[25] Q. Liu, S. Wang, Y. Zheng, Z. Luo, K. Cen, Journal of Analytical and Applied Pyrolysis 82 (2008) 170.
[26] D. Ferdous, A.K. Dalai, S.K. Bej, R.W. Thring, N.N. Bakhshi, Fuel Processing Technology 70 (2001) 9.
[27] L. Chen, X. Wu, K. Cen, Journal of Zhejiang University: Engineering science 40 (2009) 1154.
[28] D. Güllü, A. Demirbaş, Energy Conversion and Management 42 (2001) 1349.
[29] H. Haykiri-Acma, S. Yaman, S. Kucukbayrak, Fuel Processing Technology 91 (2010) 759.
[30] A. Gani, I. Naruse, Renewable Energy 32 (2007) 649.
[31] J. Piskorz, D. Radlein, D.S. Scott, Journal of Analytical and Applied Pyrolysis 9 (1986) 121.
[32] G.N. Richards, Journal of Analytical and Applied Pyrolysis 10 (1987) 251.
[33] H. Tan, Mechanism Study of Biomass Pyrolysis, Doctoral dissertation Zhejiang University 2000, in Chinese.
[34] D. Ayhan, Progress in Energy and Combustion Science 30 (2004) 219.
[35] Y. Peng, S. Wu, Transactions of China Pulp and Paper 25 (2010) 1.